

# **Chapter 4**

## **Experiments**

### **4.1 Aims**

Two experiments are designed for this thesis: (i) human-image interaction (HII) and (ii) human-humanoid interaction (HHI), in both experiments participants perform simple arm movements repetitions. Simple arm movements here means, for persons and the humanoid robot, the ideally use of one joint biomechanical degree of freedom moving at normal and faster velocities. Hence, the aims of such experiments is not only to investigate the weaknesses and robustness of RSS, UTDE, embedding parameters, RP and RQA metrics regarding different conditions presented in real-world time series data (noisiness, non-stationarity, smoothness, window size lengths and structures), but also to present experimental scenarios where one can observe how the variables that model movement variability (e.g. complexity, predictability and activity type) affect the results of nonlinear analysis (Stergiou et al., 2006; Vaillancourt and Newell, 2002, 2003).

## **Experiments**

---

### **4.2 Participants**

Twenty-three participants, from now on defined as  $pN$  where  $N$  is the number of participant, were invited for two experiments to perform simple arm movements. However, it is important to note that although the same number of participants performed the experiments, different number of participants were taken into account for each of the experiments due to either technical problems with the sensors or mistaken instructions of the experiments given to the participants.

#### **4.2.1 Human-image imitation activities**

Only six participants ( $p01, p04, p05, p10, p11, p15$ ) were considered for the experiment of Human-image imitation (HII) activities due to problems with the inertial sensors such as bluetooth disconnections and drifting of time synchronisation (Section C.1.1). The six participants for this experiment were male right-handed healthy participants and have a mean and standard deviation (SD) age of mean=19.5 (SD=0.83) years.

#### **4.2.2 Human-humanoid imitation activities**

For the experiment of human-humanoid imitation (HHI) activities, data for only twenty participants were analysed since the instructions for  $p01$ , who was the only left-handed, were mistakenly given in a way that movements were differently performed from what had been planned, and for participants  $p13$  and  $p16$  data were corrupted because of bluetooth communications problems with the sensors (Section C.1.1). With that in mind, all of the 20 participants were right-handed healthy participants, being four females and sixteen males, with a mean and standard deviation (SD) age of mean=19.8 (SD=1.39) years.

## **4.3 Equipment**

During the experiments, time series were collected with four neMEMSi Inertial Measurement Units (IMUs) with a sampling rate of 50Hz (Comotti et al., 2014). neMEMSi sensors provide tri-axial time series from the accelerometer, gyroscope and magnetometer sensors and quaternions. See Appendix C.1 for further technical information of NeMEMSi IMU sensors. With regard to the human-humanoid imitation activities, NAO, a humanoid robot from Aldebaran (Gouaillier et al., 2009), was programmed with Choregraphe to perform horizontal and vertical arm movements. See Appendix C.3 for further technical information regarding NAO.

## **4.4 Ethics**

The experiments of this thesis were conducted in November 2016 and participants confirmed reading and understanding the participant information sheet of the experiments and were able to withdraw from the experiment at any time without giving any reason. The design of the experiments adhered to the University of Birmingham regulations, data were anonymised and videos were stored only on a personal computer in accordance with the Data Protection Act 1998. Refer to Appendix D for further information about the ethics, online participation information sheets and experiment check list.

## **4.5 Experiments**

### **4.5.1 Human-image imitation activities**

In the experiment of human-image imitation (HHI), four wearable IMUs sensors were used and attached to the right hand of the participant (Figure 4.1 A,D). Then, par-

## **Experiments**

---

ticipants performed two experiments: (i) an unconstrained arm movement imitation activity where participants only receive instructions and look at images of arm movements, and (ii) a constrained experiment where participants hear a sound beat to synchronise their arm movements.

### **Arm movements following an image while not hearing a beat**

Participants received instructions to perform unconstrained upper arm movements while only looking an image for the following four activities:

- ten repetitions of horizontal arm movement at their comfortable velocity (Fig. 4.1(A, B, C)),
- ten repetitions of vertical arm movement at their comfortable velocity (Fig. 4.1(D, F, E)),
- ten repetitions of horizontal arm movement at a faster velocity than the comfortable velocity but not at their fastest velocity (Fig. 4.1(A, B, C)), and
- ten repetitions of vertical arm movement at a faster velocity than the comfortable velocity but not at their fastest velocity (Fig. 4.1(D, F, E)).

### **Arm movements following an image while hearing a beat**

Participants received instructions to perform constrained upper arm movements while listening a beat for the following four activities:

- ten repetitions of horizontal arm movement at normal velocity (Fig. 4.1(A, B, C)),
- ten repetitions of vertical arm movement at normal velocity (Fig. 4.1(D, F, E)),
- ten repetitions of horizontal arm movement at faster velocity and (Fig. 4.1(A, B, C)), and
- ten repetitions of vertical arm movement at faster velocity (Fig. 4.1(D, F, E)).

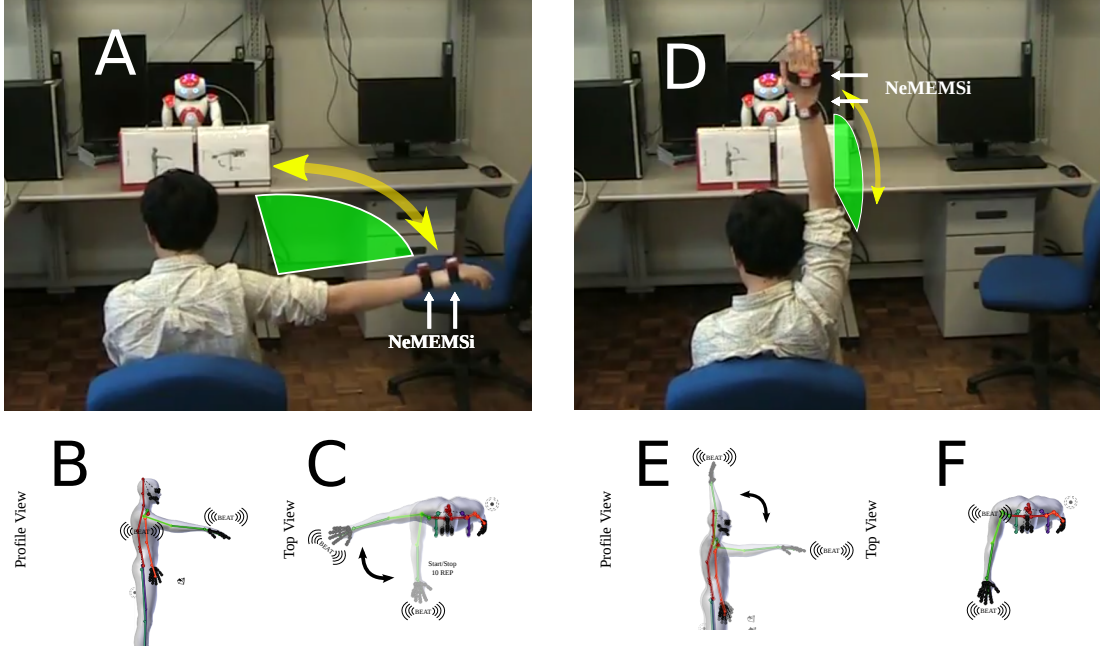


**Fig. 4.1 Human-image imitation (HII) activities.** (A) HII of horizontal arm movement, (B) image of the profile view for horizontal arm movement, (C) image of the top view for horizontal arm movement, (D) HII of vertical arm movement, (E) image of the profile view for vertical arm movement, and (F) image of the top view for vertical arm movement. (B, C, F and E) show '(((BEAT)))' to indicate the participants arm movements synchronisation when hearing a sound beat.

To visualise the time series of the previous activities, Figs 4.2 show time series using smoothed time series of the gyroscope of Y and Z axis for the sensor HS01 of participant 01. See Appendix E.1 for time series of all participants and activities.

#### 4.5.2 Human-humanoid imitation activities

NAO is commonly used in human-robot interaction activities because its affordability, performance and modularity. However, some of the limitations of NAO are related to (i) its 14 degrees of freedom (DOF) for arms and head, (ii) the range of joint movement and (iii) joint torques and velocities (Gouaillier et al., 2009). With that in mind, four NAO's arm movements were selected, such movements are controlled by the shoulder

## Experiments

---

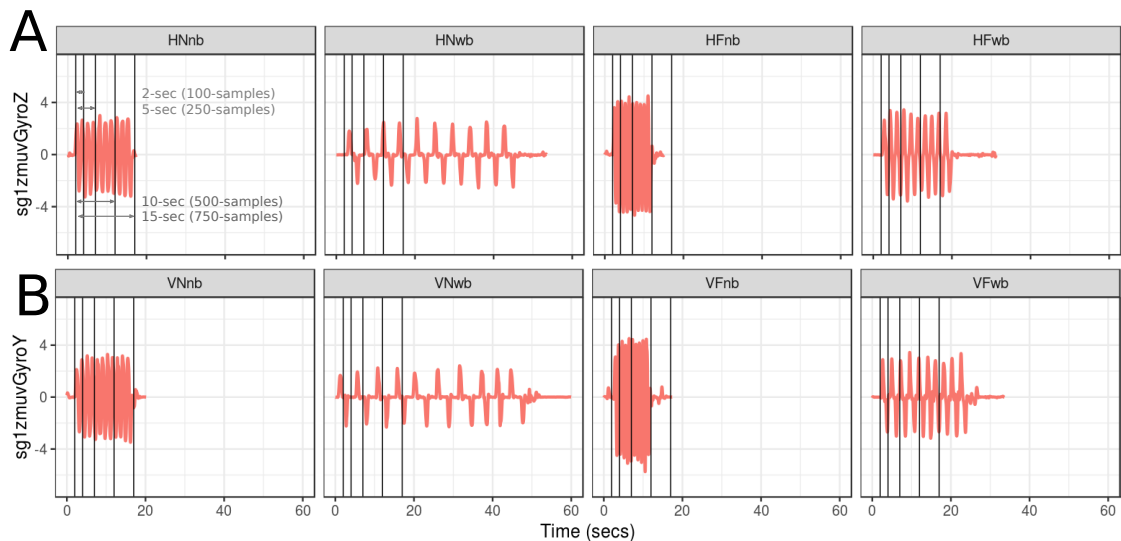


**Fig. 4.2 Time series for horizontal and vertical arm movements.** Time series of smoothed data from gyroscope sensor ( $sg1zmuvGyroZ$  and  $sg1zmuvGyroY$ ) of participant 01 with sensor HS01 for different velocity arm movements: (A) Horizontal Normal with no beat (HNnb), Horizontal Normal with beat (HNwb), Horizontal Faster with no beat (HFnb) and Horizontal Faster with beat (HFwb), and (B) Vertical Normal with no beat (VNnb), Vertical Normal with beat (VNwb), Vertical Faster with no beat (VFnb) and Vertical Faster with beat (VFwb). Additionally, (A) presents vertical lines to show window size lengths for 2-seconds (100 samples), 5-seconds (250 samples), 10-seconds (500 samples) and 15-seconds (750 samples) which are presented in (B), (C) and (D). See Appendix E.1 for time series of all participants and activities. R code to reproduce the figure is available at [\[link\]](#).

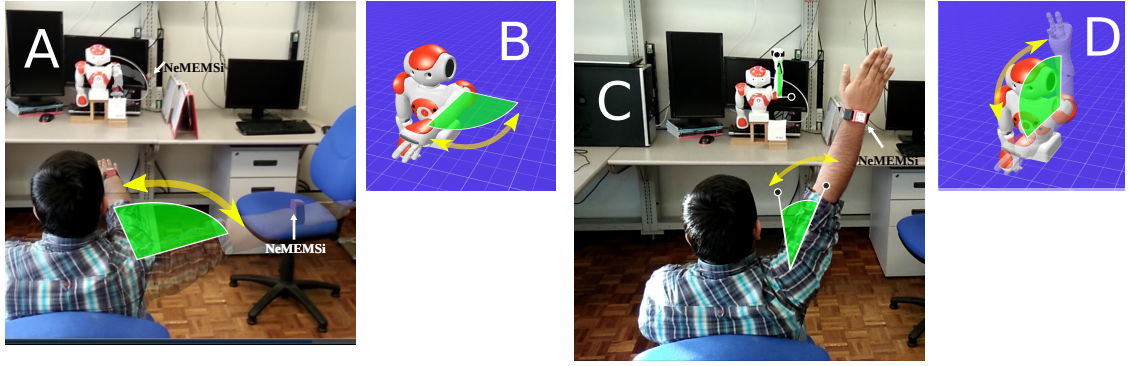


**Fig. 4.3 Human-humanoid imitation activities.** Face-to-face human-humanoid imitation (HHI) activities for (A) HHI of horizontal arm movement, (B) Humanoid performing horizontal arm movement, (C) HHI of vertical arm movement, and (D) Humanoid performing vertical arm movement.

joint for vertical and horizontal movements performed at normal and faster velocity (Figs. 4.3 B,D). See Appendix C.3 for basic information of NAO and see Gouaillier et al. (2009) for detailed information of NAO's mechanical and dynamic capabilities.

For the human-humanoid imitation (HHI) experiment four wearable IMUs sensors were used in which two sensors were attached to the right hand of the participant and two sensors were attached to the left hand of the humanoid robot (Figure 4.3 A,C). Then, in the face-to-face imitation activity, each participant was asked to imitate repetitions of simple horizontal and vertical arm movements performed by the humanoid robot in the following conditions:

- ten repetitions of horizontal arm movement at normal (HN) and faster (HF) velocity (Fig. 4.3 A), and
- ten repetitions of vertical arm movement at normal (VN) and faster (VF) velocity (Fig. 4.3 C).

The duration of number of samples for NAO's arm movements were defined by normal and faster velocities of NAO's shoulder joint (Figs. 4.3 B,D). Hence, the duration for one repetition of the horizontal arm movement at normal velocity, HN,

## Experiments

---

is about 5 seconds considering that each repetition last around 250 samples. For horizontal arm movement at faster velocity, HF, each repetition were performed in around 2 seconds which correspond to 90 samples of data. The vertical arm movement at normal velocity, VN, were performed in 6 seconds which is around 300 samples of data. For vertical arm movement at faster velocity, VF, each repetition lasts about 2.4 seconds which correspond to 120 samples of data. To visualise the distinction between normal and faster velocity for horizontal and vertical arm movements, Fig 4.4 shows smoothed time series for axes Z and Y of the gyroscope sensors with four window lengths: 2-sec (100-samples), 5-sec (250-samples), 10-sec (500-samples) and 15-sec (750-samples). See Appendix F.1 for time series of all participants and activities.

## 4.6 Processing of time series

### 4.6.1 Raw time-series

For this thesis, analysis of time series is only with the accelerometer and gyroscope of the IMU sensors. The justification for that is because Shoaib et al. (2016) provided evidence of an improvement in recognition activities when only combining data from accelerometer and gyroscope. The time-series data for magnetometer and quaternions are left for future investigations as these might create additional variations because of magnetic disturbances.

Time series from the accelerometer are defined by triaxial time series  $A_x(n)$ ,  $A_y(n)$ ,  $A_z(n)$  which forms the matrix  $\mathbf{A}$  (Eq. 4.1), and the same for data from the gyroscope which is defined by triaxial time-series of  $G_x(n)$ ,  $G_y(n)$ ,  $G_z(n)$  representing the matrix  $\mathbf{G}$  (Eq. 4.2). Both triaxial time series of each sensor,  $a$  and  $g$ , are denoted with its respective axes subscripts  $x, y, z$ , where  $n$  is the sample index and  $N$  is the same maximum length of all axes for the time series. Matrices  $\mathbf{A}$  and  $\mathbf{G}$  are represented as

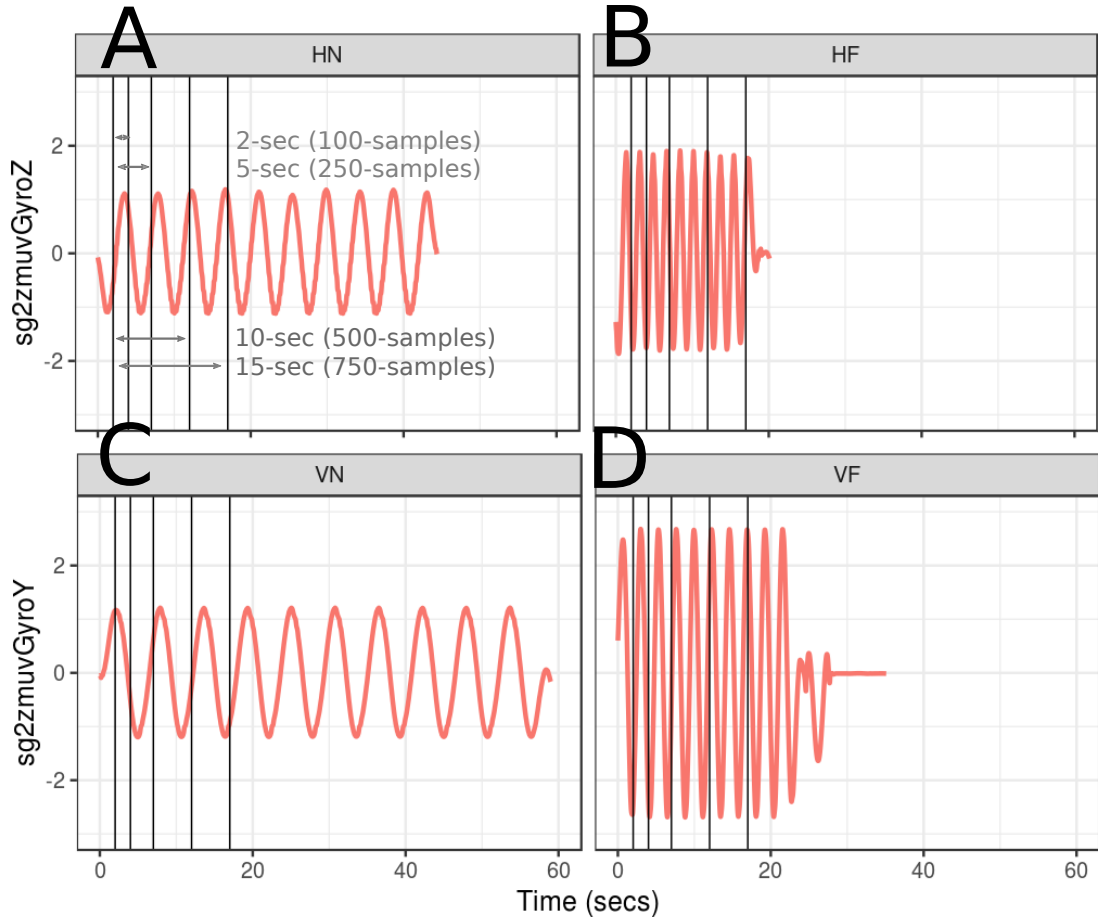


**Fig. 4.4 Time series duration of horizontal and vertical arm movements.** Time series of smoothed data from gyroscope sensor (sg1zmuvGyroZ and sg1zmuvGyroY) of NAO with sensor HS01 for different velocity arm movements: (A) Horizontal Normal arm movement, HN, (B) Horizontal Faster arm movement, HF, (C) Vertical Normal arm movement, VN, and (D) Vertical Faster arm movement, VF. Additionally, (A) presents vertical lines to show window size lengths for 2-seconds (100 samples), 5-seconds (250 samples), 10-seconds (500 samples) and 15-seconds (750 samples) which are presented in (B), (C) and (D). See Appendix F.1 for time series of all participants and activities. R code to reproduce the figure is available at [\[link\]](#).

## Experiments

---

follow

$$\mathbf{A} = \begin{pmatrix} A_x(n) \\ A_y(n) \\ A_z(n) \end{pmatrix} = \begin{pmatrix} a_x(1), a_x(2), \dots, a_x(N) \\ a_y(1), a_y(2), \dots, a_y(N) \\ a_z(1), a_z(2), \dots, a_z(N) \end{pmatrix}, \quad (4.1)$$

$$\mathbf{G} = \begin{pmatrix} G_x(n) \\ G_y(n) \\ G_z(n) \end{pmatrix} = \begin{pmatrix} g_x(1), g_x(2), \dots, g_x(N) \\ g_y(1), g_y(2), \dots, g_y(N) \\ g_z(1), g_z(2), \dots, g_z(N) \end{pmatrix}, \quad (4.2)$$

where  $n$  is the sample index and  $N$  is the same maximum length of all axes for the time series.

### 4.6.2 Postprocessing time-series

After the collection of raw time-series from four NeMEMsi sensors, time synchronisation alignment and interpolation were performed in order to create time series with same length and synchronised time. See Appendix C.2 for technical information about the IMU sensors and time synchronisation process.

### 4.6.3 Window size of time-series

With regard to the window size, Shoaib et al. (2016) compared seven window lengths (2, 5, 10, 15, 20, 25, 30 seconds) and tested a combination of inertial sensors (accelerometer, gyroscope and linear acceleration sensor) for activity recognition of repetitive activities (walking, jogging and biking) and less repetitive activities (smoking, eating, giving a talk or drinking a coffee). Shoaib et al. (2016) concluded that the increase of window size improved the recognition of complex activities (i.e. less repetitive activities which mainly involve random hand gestures). With that in mind, four window sizes were selected for each of the activities, which are mainly repetitive, in this thesis: 2-s window (100 samples), 5-s window (250 samples), 10-s (500 samples) and 15-s window (750

samples). Figures 4.2 and 4.4 illustrate vertical lines to show four window lengths which were chosen in order to cover a total time of 15 seconds (750 samples) for either (i) eight activities in human-image imitation or (ii) four activities in human-humanoid imitation. Figures 4.2 and 4.4 also show the starting point of time-series data from 2 seconds (100 samples) in order to avoid picking time-series data that do not correspond to the experiment (i.e., any movements before the experiment). The latter statement is important for the application of nonlinear analysis methods as picking dynamics of time-series data that do not correspond to the activity will therefore produce different results to the ones that only consider the duration of the activity.

### 4.6.4 Normalization of time-series

Time series are normalised to have zero mean and unit variance using sample mean and sample standard deviation (Ioffe and Szegedy, 2015). The sample mean and sample standard deviation using  $x(n)$  is given by

$$\mu_{x(n)} = \frac{1}{N} \left( \sum_{i=1}^N x(i) \right), \quad \sigma_{x(n)} = \sqrt{\frac{\sum_{i=1}^N (x(i) - \mu_{x(n)})^2}{N-1}}, \quad (4.3)$$

then the normalised data,  $\hat{x}(n)$ , is computed as follows

$$\hat{x}(n) = \frac{x(n) - \mu_{x(n)}}{\sigma_{x(n)}}. \quad (4.4)$$

### 4.6.5 Smoothing time-series

Applying low-pass filters is a common way to either capture low frequencies (below 15 Hz) that represent 99% of the human body energy or to get the gravitational and body motion components of accelerations (below 0.3 Hz) (Anguita et al., 2013). However, filtering such information can cut-off frequencies that are important for the

## **Experiments**

---

conservation of (i) the original properties of raw time-series data and (ii) the structure of the time-series data in terms of width and heights. In addition to that, arm movements of NAO can sometimes produce jerky movements due to: (i) the control of dynamic response (fast acceleration/deceleration), (ii) the stiffness of the gear mechanism, or (iii) the high frequencies of oscillations because of resonances (see Gouaillier et al. (2009) for NAO's mechanical and dynamic capabilities). Hence, instead of cutting out frequencies with a low-pass filter for the experiments in the context of human-robot interaction, this thesis considers the application of Savitzky-Golay filter to smooth time series data. The latter statement might give insight into the effect of smoothness of real-world time series data for nonlinear analysis methods.

Savitzky-Golay filter is based on the principle of moving window average which preserves the area under the curve (the zeroth moment) and its mean position in time (the first moment) but the line width (the second moment) is violated and that results, for example, in the case of spectrometric data where a narrow spectral line is presented with reduced height and width (Press et al., 1992). The aim of Savitzky-Golay filtering is hence to find the filter coefficients  $c_n$  that preserve higher momentums which are based on local least-square polynomial approximations (Press et al., 1992; Savitzky and Golay, 1964; Schafer, 2011). Therefore, Savitzky-Golay coefficients are computed using an R function `sgolay(p,n,m)` where  $p$  is the filter order,  $n$  is the filter length (must be odd) and  $m$  is the  $m$ -th derivative of the filter coefficients (signal R developers, 2014). Smoothed signal is represented with a tilde over the original signal:  $\tilde{x}(n)$ .